ARMY RESEARCH LABORATORY

Synthesis and Characterization of DNase 1-Stabilized Gold Nanoclusters

by Abby L West, Mark H Griep, Daniel P Cole, and Shashi P Karna

ARL-TR-7129 October 2014

NOTICES

Disclaimers

The findings in this report are not to be construed as an official Department of the Army position unless so designated by other authorized documents.

Citation of manufacturer's or trade names does not constitute an official endorsement or approval of the use thereof.

Destroy this report when it is no longer needed. Do not return it to the originator.

Army Research Laboratory
Aberdeen Proving Ground, MD 21005-5069

ARL-TR-7129 **October 2014**

Synthesis and Characterization of DNase 1-Stabilized Gold Nanoclusters

Abby L West, Mark H Griep, and Shashi P Karna
Weapons and Materials Research Directorate, ARL

Daniel P Cole
Vehicle Technology Directorate, ARL

REPORT DOCUMENTATION PAGE	Form Approved OMB No. 0704-0188

1. REPORT DATE *(DD-MM-YYYY)*	2. REPORT TYPE	3. DATES COVERED (From - To)
October 2014	Final	November 2013–January 2014

4. TITLE AND SUBTITLE
Synthesis and Characterization of DNase 1-Stabilized Gold Nanoclusters

5a. CONTRACT NUMBER

5b. GRANT NUMBER

5c. PROGRAM ELEMENT NUMBER

6. AUTHOR(S)
Abby L West, Mark H Griep, Daniel P Cole, and Shashi P Karna

5d. PROJECT NUMBER

5e. TASK NUMBER

5f. WORK UNIT NUMBER

7. PERFORMING ORGANIZATION NAME(S) AND ADDRESS(ES)
US Army Research Laboratory
ATTN: RDRL-WMM-A
Aberdeen Proving Ground, MD 21005-5069

8. PERFORMING ORGANIZATION REPORT NUMBER
ARL-TR-7129

9. SPONSORING/MONITORING AGENCY NAME(S) AND ADDRESS(ES)

10. SPONSOR/MONITOR'S ACRONYM(S)

11. SPONSOR/MONITOR'S REPORT NUMBER(S)

12. DISTRIBUTION/AVAILABILITY STATEMENT
Approved for public release; distribution is unlimited.

13. SUPPLEMENTARY NOTES

14. ABSTRACT
DNase 1-stabilized gold nanoclusters (DNase 1 AuNCs) were synthesized with multiple energy levels in a metal-concentration-dependant fashion. From multiple characterization techniques including fluorescence spectroscopy, high-resolution transmission electron microscopy and X-ray photoelectron spectroscopy, we assigned 2 reaction products to contain pure populations of clusters with core sizes of 8 and 25 Au atoms for the products where 10- and 2.5-mM HAuCl4 was used in the reaction, respectively, and 2 reaction products to contain either mixtures of the Au8 and Au25 clusters or Au nanoparticles (AuNPs) dependent upon the initial Au concentration. An initial HAuCl4 concentration of 5 mM produced a small amount of AuNPs but no NCs, while an initial concentration of 0.5-mM HAuCl4 resulted in a mixture of Au8 and Au25 clusters with a higher percentage of Au25 clusters. The DNase 1 Au8NCs exhibiting blue fluorescence have an excitation and emission maxima of 390 and 460 nm, respectively, whereas the DNase 1 Au25NCs are red-emitting and have an excitation and emission maxima of 490 and 640 nm, respectively.

15. SUBJECT TERMS
protein-stabilized NCs, DNase 1, bionano hybrids, gold nanoclusters, fluorescence spectroscopy

16. SECURITY CLASSIFICATION OF:			17. LIMITATION OF ABSTRACT	18. NUMBER OF PAGES	19a. NAME OF RESPONSIBLE PERSON
a. REPORT	b. ABSTRACT	c. THIS PAGE			Shashi P Karna
Unclassified	Unclassified	Unclassified	UU	26	19b. TELEPHONE NUMBER (*Include area code*) 410-306-0723

Contents

List of Figures

List of Tables

Acknowledgments

The authors would like to thank Victor Rodriguez Santiago for the X-ray photoelectron spectroscopy. We also acknowledge the support of the Maryland NanoCenter and its NispLab for transmission electron microscopy analysis. The NispLab is supported in part by the National Science Foundation as a Materials Research Science and Engineering Center Shared Experimental Facility. The authors would also like to thank Michael Sellers and Joshua Martin for aid and input on this work. Abby West acknowledges the receipt of an US Army Research Laboratory-Oak Ridge Associated Universities Postdoctoral Associateship.

INTENTIONALLY LEFT BLANK.

1. Introduction

The labeling of biological molecules like protein or DNA has been a large thrust in various clinical applications including targeted drug delivery, cancer imaging, radiotherapy, and cardiovascular disease. Commercially available fluorophores are limited by several inherent deficiencies such as photobleaching, biotoxicity, native function perturbation of the labeled biomolecule, and toxic synthesis protocols. For example, organic dyes such as fluorescein isothiocyanate (FITC) green and diamidino-2-phenylindole (DAPI) blue are easily photobleached with FITC, exhibiting 20% fluorescence after just 2 min while DAPI fluorescence is minimal after 5 min.[1,2] Fluorescent proteins such as green fluorescent protein and yellow fluorescent protein are nicely biocompatible. However, the large size of the tag often disrupts the native function of the labeled protein including protein-protein interactions and cellular transport.[3]

Semiconductor quantum dots (QDs) are very attractive labels for biological processes, as they have several advantageous qualities including photostability, high quantum yield, small size, and a narrow emission profile. QDs are composed of a single crystal of a semiconductor material such as cadmium selenide (CdSe) and are roughly a few nanometers in diameter.[4] The diameter of the QD crystal can be explicitly controlled with temperature and duration variations in the synthesis protocol.[4] As QDs are a few nanometers in diameter, they are smaller than the Bohr exciton radius, thus energy levels within the crystal are quantized and directly proportional to the size of the crystal. Ultimately, QDs exhibit unique, size-dependant absorbance and emission profiles that allow for greater diversity in biological labeling applications.[4] However, QDs have several important drawbacks such as photoblinking due to imperfections on the crystal surface.[5] In addition, as materials like CdSe are inherently toxic, large capping molecules must be added to the QD exterior to ensure biocompatibility. Furthermore, this process leads to an increase of the QD diameter to 10–14 nm, which is quite large relative to the size of proteins leading to the disruption of normal protein function.[6]

Noble metal nanoclusters (NCs) are also very attractive within the fields of biosensing, biodetection, and biomedicine, as they offer the necessary functionalities of traditional semiconductor QDs, including tunable emission, ease of conjugation, extended photostability, and high quantum yield.[7,8] In addition, NCs also surpass traditional quantum dots in several notable areas such as 1) being composed of nontoxic/biocompatible materials, 2) green synthesis routes, 3) function with a fraction of the metal content, 4) considerably reduced size for enhanced cellular uptake, and 5) exhibit demonstrated renal evacuation efficacy. These added unique properties make noble metal NC research an area of great interest with numerous applications in a variety of research fields, from biologics to optics and photovoltaics.[8–17] NCs are small clusters of metal atoms ranging from fewer than 10 to several hundred atoms with a

diameter of less than 2 nm.[8] NCs exhibit quantized energy fluorescence similar to QDs due to the small diameter as opposed to the plasmonic transitions exhibited by noble metal nanoparticles (Fig. 1).[18,19] For instance, gold nanoclusters (AuNCs) experience a blue shift in the emission wavelength as they decrease in size; i.e., NCs composed of 5, 13, and 25 Au atoms exhibit blue, green, and red fluorescence, respectively.[20] NCs can be generated in a variety of ways ranging from purely synthetic to fully biostabilized and several methods that fall between.[7,8,16,18,19,21–25]

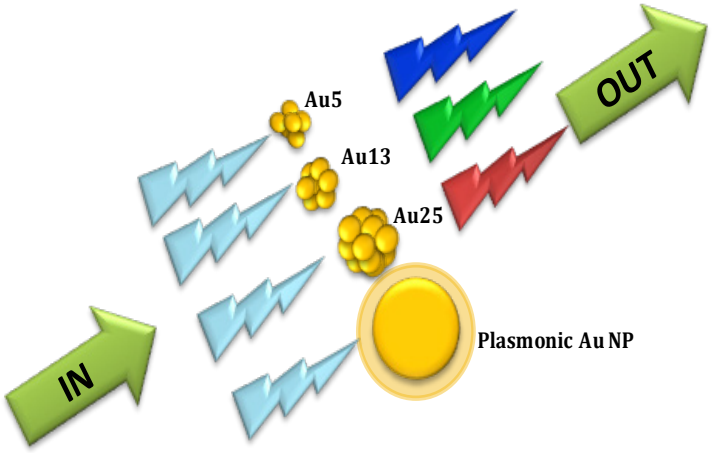

Fig. 1 Comparison of distinct fluorescence emissions exhibited by AuNCs to the plasmonic transitions of AuNCs

Protein-mediated synthesis of noble metal NCs is particularly interesting because these NCs exhibit the highest level of biocompatibility, as they are synthesized by biological molecules. Furthermore, protein-stabilized NCs can be used for a wide range of sensing applications either by harnessing the inherent native function of the protein or by exploiting the effect of the scaffold protein's environment on NC fluorescence.[8,13,26] Protein-stabilized NC synthesis has been demonstrated with several proteins including BSA, apo-transferrin, pepsin, lysozyme, insulin, CRABP, horseradish peroxidase, and others.[9,20,27–32] In addition, a few proteins such as human apo-transferrin, insulin, and horseradish peroxidase have been shown to retain native function after AuNC encapsulation and have subsequently been used as biosensors.[28,30,33] Here we present a new approach for biomolecule mediated synthesis of AuNCs. We have for the first time used DNase 1 to synthesize AuNCs of multiple energy levels. The NCs show intense blue and fluorescence, exhibit long-term stability, and are resistant to photobleaching.

2. Materials and Methods

All materials for this study were purchased from Sigma Aldrich.

2.1 Synthesis of DNase 1-Stabilized AuNCs

DNase 1 from bovine pancreas was resuspended in Milli Q water at a concentration of 20 mg/mL. Added to 2 mL of protein solution was 2 mL of aqueous solution of $HAuCl_4$ (20, 10, 5, or 1 mM) under vigorous stirring at 37 °C (see Table). After 5 min, 200 μL of NaOH (1 M) was added to raise the pH to approximately 12 for the 1, 5, and 10-mM $HAuCl_4$ samples while 400 μL of NaOH (1M) was required to obtain a pH of 12 for the 20-mM $HAuCl_4$ sample due to the increase concentration of Au ions. The increase in pH activates the reductive activity of the tyrosine residues within the protein. The various protein/Au mixtures were then left to react for 12 h. The solution changed in color from light yellow to various shades of deeper yellow-gold over the course of the reaction. A parallel experiment was set up with 20-mg/mL protein alone as a control. This solution was initially clear and remained so throughout the course of the incubation.

Table Representation of the different reaction conditions examined in this study

Trial No.	Stock (Protein) (mg/mL)	Stock (Au) (mM)	Final (Au) (mM)	1-M NaOH Added (μL)
1	20	20	10	400
2	20	10	5.0	200
3	20	5	2.5	200
4	20	1	0.5	200

2.2 Ultraviolet-Visible Spectroscopy

Ultraviolet (UV)-Visible measurements were taken with a Nanodrop 2000c over a wavelength range of 200–800 nm.

2.3 Fluorescence Spectroscopy

The fluorescence emission spectra were collected with a Horiba Jobin Yvon FluoroLog-3 spectrofluorometer with maximum excitation wavelengths of 365, 395, 450, and 488 nm. The emission spectrum was measured from 400 to 700 nm. The fluorescence excitation spectra were obtained through the measurement of 2 different maximum emission wavelengths, 460 and 630 nm.

2.4 X-ray Photoelectron Spectroscopy Analysis

Near-surface compositional depth profiling of the as-deposited coatings was performed using the Kratos Axis Ultra X-ray photoelectron spectroscopy (XPS) system, equipped with a hemispherical analyzer. A 100-W monochromatic Al Kα (1486.7-eV) beam irradiated a

1- × 0.5-mm sampling area with a take-off angle of 90°. The base pressure in the XPS chamber was held between 10^{-9} and 10^{-10} Torr. Elemental high-resolution scans for Au_{4f} core level were taken in the constant analyzer energy mode with 160-eV pass energy. The sp^3 C_{1s} peak was used as reference for binding energy calibration.

2.5 Transmission Electron Microscopy

Morphological studies and elemental characterization of the materials were performed using a field emission transmission electron microscope (TEM) (JEOL JEM-2100F TEM/STEM) operated at 200 kV. The TEM system was equipped with an energy dispersive spectroscopy system (INCA 250, Oxford Instruments) and imaging filter (Gatan). Microscopy samples were prepped for analysis through the following steps: 1) bulk material ground up using a mortar and pestle, 2) particles dispersed in deionized water and bath sonicated for 15 min, 3) solution pipetted onto TEM grids (ultrathin carbon film on holey carbon support film, 300 mesh, Ted Pella, Inc.), followed by removal of excess solution using a filter paper, and 4) samples allowed to dry in air at room temperature for over 2 hr.

3. Results and Discussion

Traditional chemical reduction and polymer etching techniques for AuNC synthesis require the addition of harsh and environmetally unfriendly reducing agents such as soduim borohydride and tetrabutylammonium borohydride. These agents are necessary to reduce the Au (III) in solution to the final oxidation states of Au (I) and Au (0) that comprise the NC. Ying and coworkers were the first to use the theory of biomineralization to create a biostabilized AuNC using the amino acids within BSA as the exclusive reducing agent during NC synthesis.[27] The amino acid tyrosine has the ability to reduce Au in an alkaline environment as tyrosine residues have a pKa value of 10.07 and contain a phenolic group.[34] Therefore, raising the pH to approximately 12 during synthesis ionizes the phenol and activates the reducing capability of these residues. As DNase 1 has 15 tyrosine residues, we hypothesized that the protein may be able to serve as a molecular scaffold for NC synthesis. DNase 1 from bovine pancreas was used as the template for NC synthesis in this study. AuNC encapsulation by DNase 1 was completed after 12 h of incubation at 37 °C. The size of the resultant NC depended upon the initial Au (III) concentration used in the synthesis reaction. The use of a final concentration of 10-mM Au (III) chloride salt produced NCs comprised of 5–8 atoms while the use of 2.5-mM Au (III) chloride produced NCs containing 25 atoms. Multiple characterization techniques were employed to determine the size and properties of the AuNC encapsulated within the protein.

3.1 Gold (III)-Concentration-Dependant Synthesis of DNase 1-Stabilized AuNCs

DNase 1-stabilized AuNCs with varied peak emission wavelengths were synthesized by incubating 20-mg/mL enzyme with a range of Au (III) chloride salt from 10- to 0.5-mM final concentration. Following a subsequent increase in pH and 12-h incubation time, DNase 1-stabilized AuNCs with blue, gray, red, and pink fluorescence could be observed with UV illumination from the 10-, 5-, 2.5-, and 0.5-mM $HAuCl_4$ reactions, respectively (Fig. 2). The reaction products that emit strong blue and red fluorescence are thought to be homogenous solutions of DNase 1-stabilized $Au_{5/8}$ and Au_{25} NCs. As gray and pink are not true fluorescent colors, we hypothesized that the gray- and pink-emitting samples contain mixtures of AuNC sizes; the gray-emitting (5-mM) reaction containing more $Au_{5/8}$ clusters while the pink-emitting (0.5-mM) contains more Au_{25} clusters.

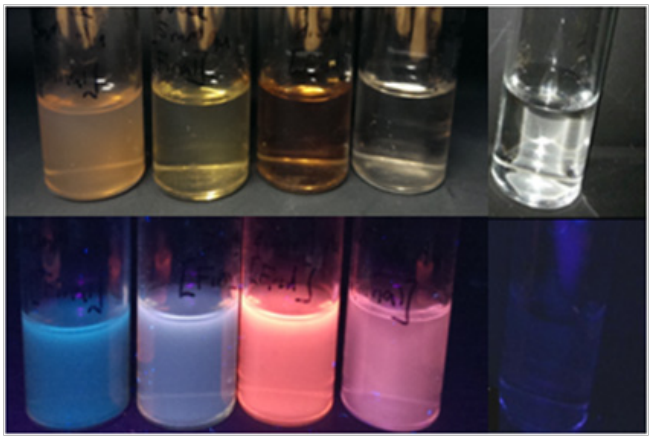

Fig. 2 Fluorescence emission of DNase 1 AuNCs. Visible (top) and UV (bottom) illumination of DNase AuNCs (left to right: 10-, 5-, 2.5-, 0.5-, and 0-mM Au [III] added).

3.2 Photophysics of DNase 1-Stabilized AuNC

To fully characterize and understand the multiple forms of DNase 1-stabilized AuNCs, it was necessary to determine the photophysics of the nano-bio hybrids. Complete emission and excitation spectrums were collected for the 4 reactions and are highlighted in Figs. 3–6. The blue-emitting clusters synthesized with 10-mM Au(III) exhibited a maximum emission wavelength of 460 nm and a maximum excitation wavelength of 395 nm when monitoring the 460-nm peak fluorescence. Both the excitation and emission spectrums were decidedly pure and had no other peaks. According to the study presented by Kawasaki et al. involving the pH dependant synthesis of blue-, green-, and red-emitting AuNCs, a peak emission wavelength of 460 nm is consistent with Au clusters comprised by 5 or 8 atoms.[20] In addition, a peak emission wavelength of 460 nm is also consistent with data for lysozyme Au_8 clusters studied by Chen and Tseng.[35]

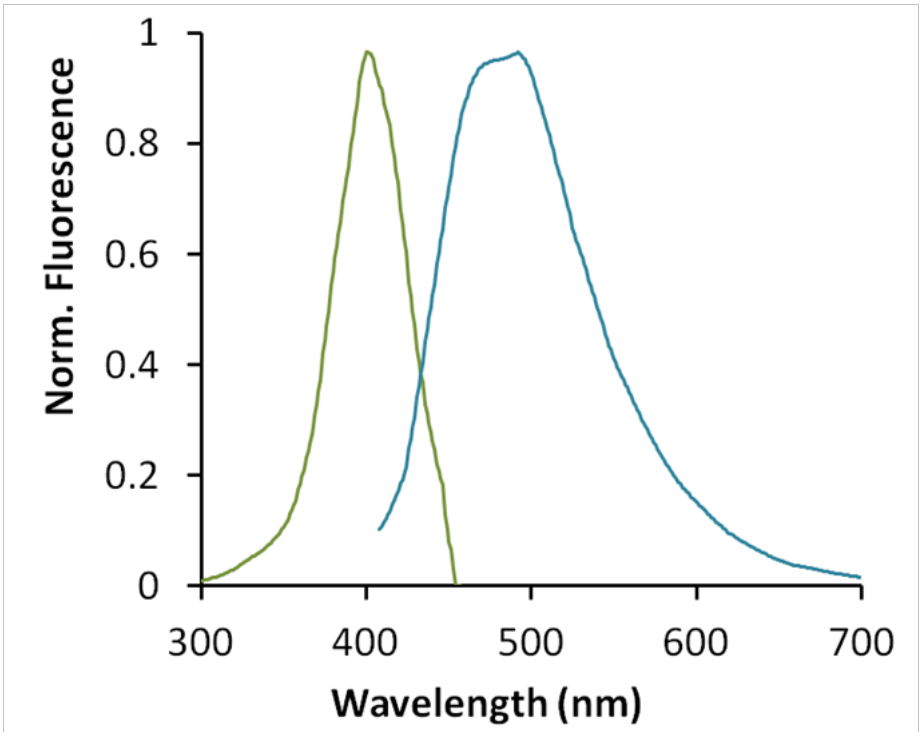

Fig. 3 Excitation (green) and emission (blue) spectra of DNase 1 AuNCs synthesized with 10-mM $HAuCl_4$

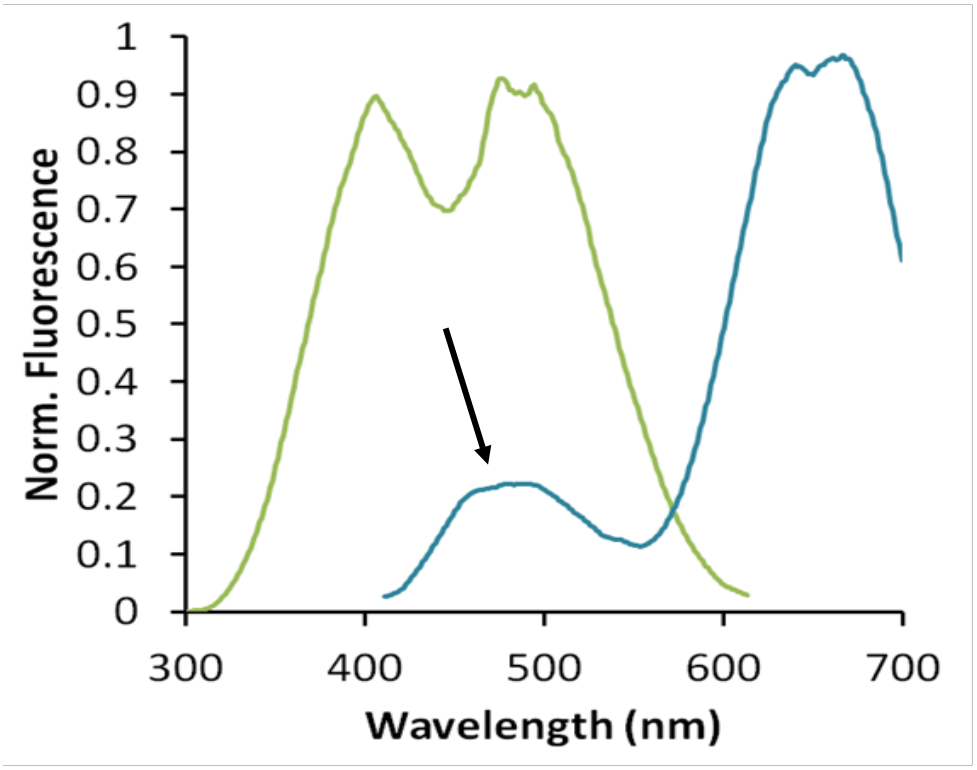

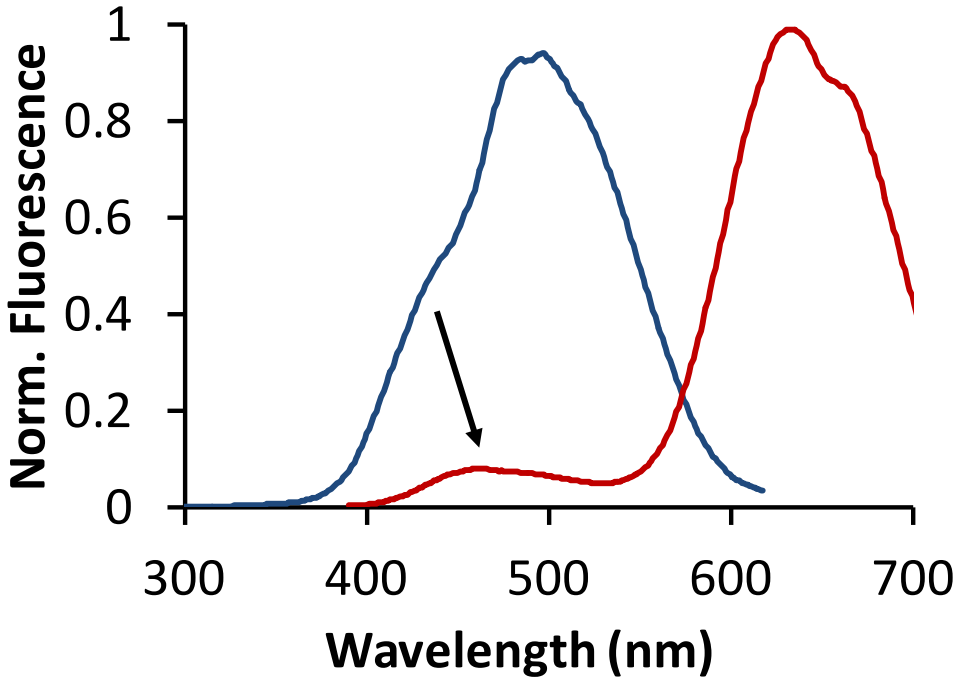

Fig. 4 (top) Excitation (green) and emission (purple) spectra of DNase 1 AuNCs synthesized with 2.5-mM $HAuCl_4$. (bottom) Excitation (blue) and emission (red) of BSA Au_{25}NCs.

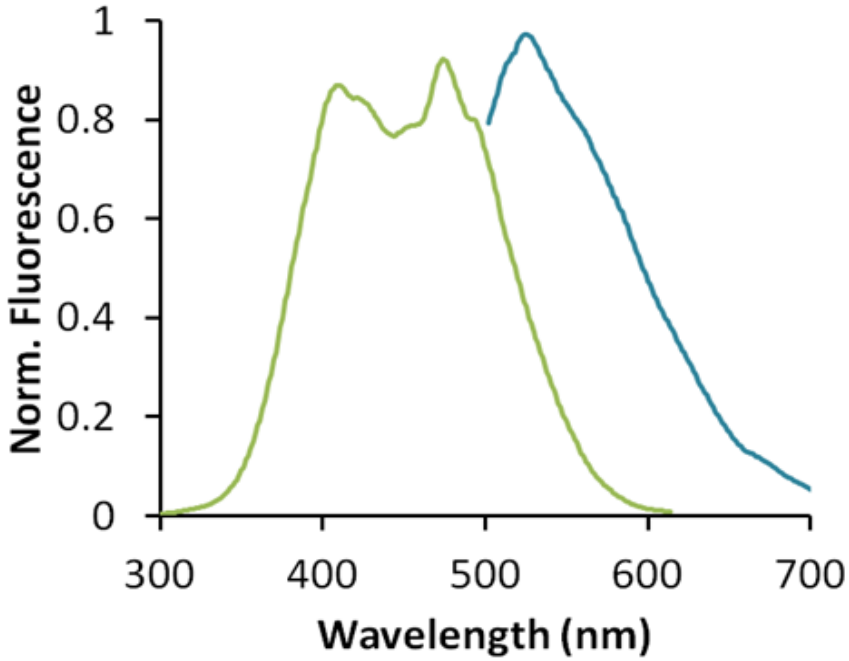

Fig. 5 Normalized fluorescence excitation and emission spectrum of DNase 1 AuNCs synthesized with 5-mM $HAuCl_4$

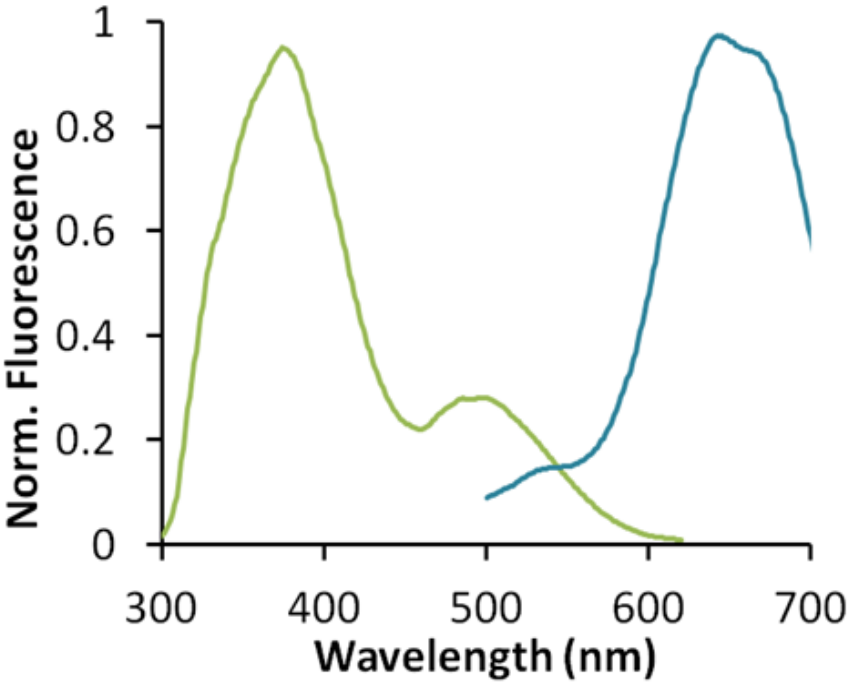

Fig. 6 Normalized fluorescence excitation and emission spectrum of DNase 1-AuNCs synthesized with 0.5-mM $HAuCl_4$

The red-emitting clusters synthesized with 2.5-mM Au exhibited peak fluorescence at 637 nm. Like the blue-emitting clusters, the emission spectrum of the red fluorescent clusters is of high purity with only a small contaminating peak at 460 nm. Compared with other published protein-stabilized Au_{25} clusters, the maximum emission wavelength for the red-emitting DNase 1 AuNCs is highly similar to the other published values, such as BSA (640 nm), lysozyme (657 nm), horseradish peroxidase (650 nm), and pepsin (640 nm). In publications where the full emission spectrum is included (lysozyme and horseradish peroxidase), a weak 460-nm signal can also be observed. Interestingly, DNase 1 Au_{25}NCs show dual excitation peaks at 395 and 460 nm (λ_{em} 637 nm). Further study is necessary to fully understand the presence of the split excitation peak, but the duality could be attributed to the minor emission peak located at 460 nm. A comparison of the excitation spectra for other protein-stabilized Au25NCs is necessary to fully understand if this is a consistent phenomenon or unique to the DNase 1-stabilized Au_{25}NCs; however, no published excitation spectra could be located for the known Au_{25} clusters. Therefore, to determine if the observed excitation peak duality was unique to DNase 1, we prepared red-emitting BSA Au_{25}NCs (λ_{em} 637 nm). The BSA Au_{25}NC excitation spectrum lacks 2 completely distinct peaks but rather has a main peak at 495 nm and a shoulder present at 410 nm. Added comparison of the emission spectra (λ_{ex} 395 nm) shows a much lower intensity 460-nm peak for the BSA Au_{25}NCs than the DNase 1 Au25NCs, lending extra support to the higher energy/shorter wavelength excitation peak being attributed to the 460-nm emission peak.

As predicted by visual inspection, the 5- and 0.5-mM Au (III) synthesis reactions appear to be nonoptimized conditions for NC synthesis. Fluorescence data for the 5-mM sample shows a very low signal strength that is visible only when the data are normalized (Fig. 5 versus Fig. 7). The emission curve does not have a true peak and thus does not indicate the presence of NCs. However, the “pink” fluorescent clusters do show a fluorescent signature and appear to consist of a low quantity of Au_{25}NCs (Fig. 6).

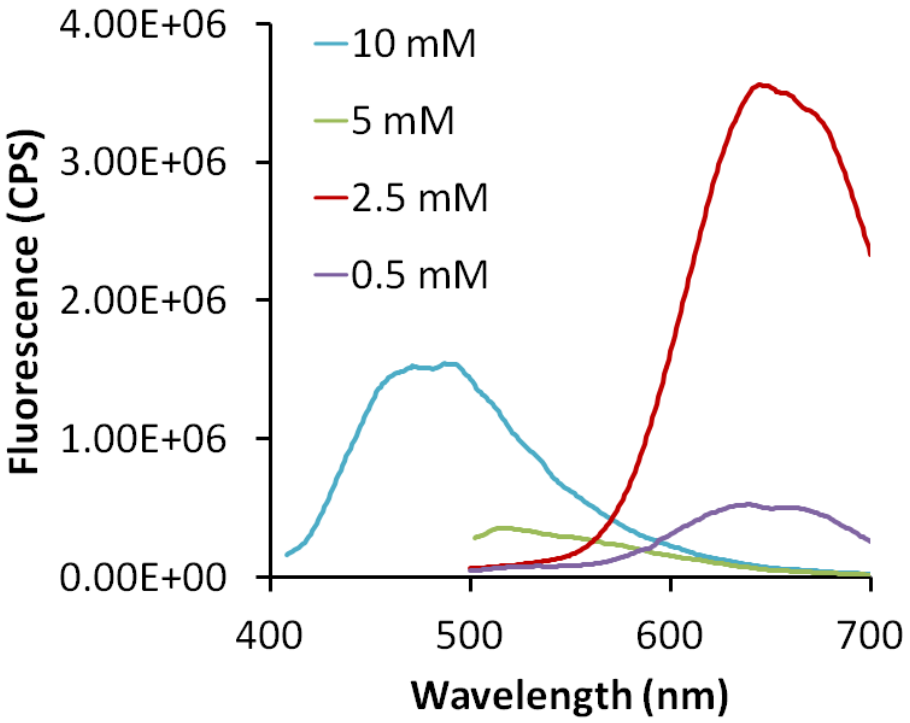

Fig. 7 Fluorescence emission spectra of the various DNase 1 AuNC synthesis products

3.3 TEM Analysis of DNase 1-Stablized AuNCs

The various DNase 1 AuNCs were characterized by both high-resolution (HR)-TEM and XPS to determine the size and oxidation states of the clusters. The HR-TEM data for the blue-emitting clusters showed a homogenous population of 1-nm and smaller clusters (Fig. 8, top left). These results are in agreement with previously published data for the lysozyme- and pepsin-stabilized Au8 clusters.[20,35] Comparing the HR-TEM data for the red-emitting DNase 1 AuNCs (Fig. 8, bottom left) to other known protein-stabilized Au_{25}NCs such as BSA,[27] pepsin,[20] lysozyme,[28] and apo-transferrin[29] showed very high similarity. These data lend further support to the blue- and red-emitting DNase AuNCs being comprised of 8 and 25 atoms, respectively. To determine if the 5- and 0.5-mM products actually contained NCs, HR-TEM was conducted. As shown in Fig. 8, the 5-mM sample did not contain any NCs, but a few large (10- to 20-nm) particles were found. The 0.5-mM sample did contain a few NCs around 2 nm in size. This finding is in agreement with the weak red fluorescence observed in the emission spectrum.

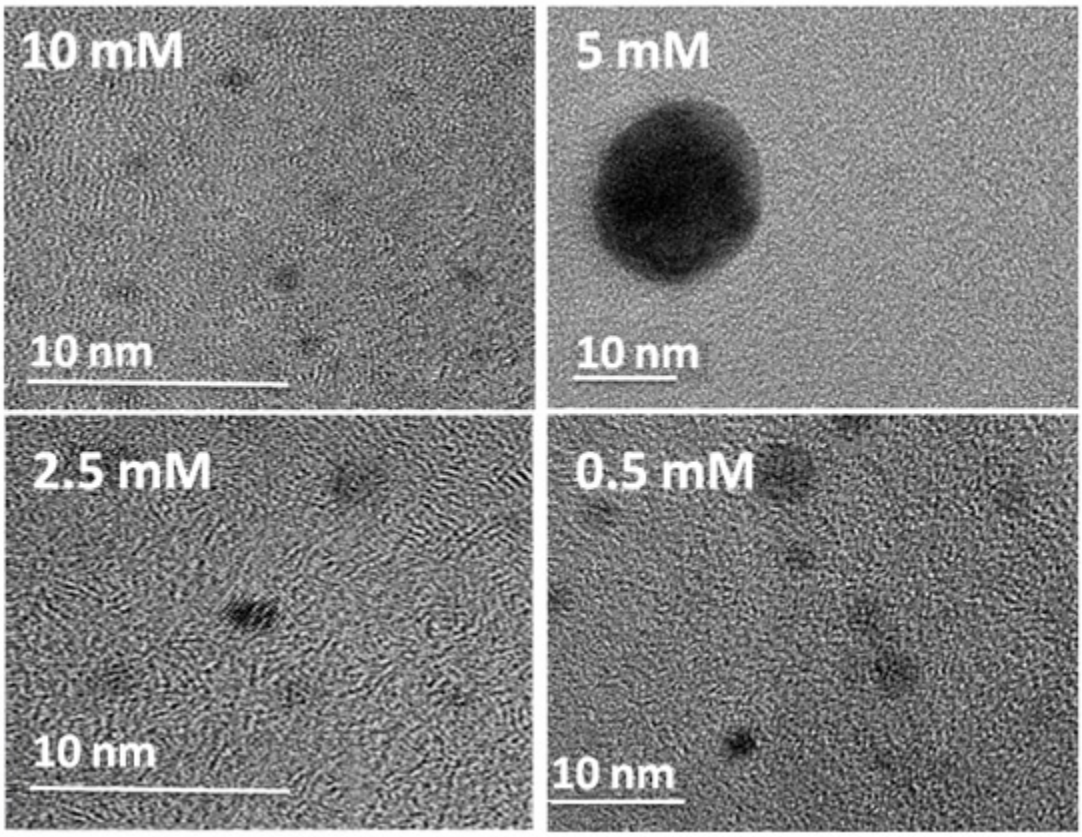

Fig. 8 HR-TEM images of the various DNase 1 AuNC synthesis products

3.4 XPS Analysis of DNase 1-Stabilized AuNCs

Following HR-TEM analysis, XPS was conducted to determine the ratio of Au (I) ions the form the shell of the clusters and Au (0) that forms the core of the cluster. The ratio of Au (I) to Au (0) should decrease as the cluster core size increases (i.e., from Au_8 to Au_{25}).[20,35] For example, lysozyme Au_8 clusters are completely comprised of elemental Au [Au (0)] with no Au (I) present on the surface.[35] As such, the DNase 1 Au_{25}NCs should have a higher percentage of oxidized metal than the DNase 1 Au_8NCs. As shown in Fig. 9, the DNase 1 Au_{25}NC XPS spectra of Au_{4f} spectra were fitted and confirm the presence of 2 distinct doublet $Au_{4f}7/2$ peaks at 84 and 85.2 eV, corresponding to Au (0) and Au (I), respectively, and show a higher percentage of Au (I) than elemental metal as expected. However, we were unable to successfully acquire XPS spectra of any of the remaining DNase 1 AuNC synthesis products. It is possible that the XPS instrument was unable to resolve the small clusters or that the sample degraded upon X-ray exposure.

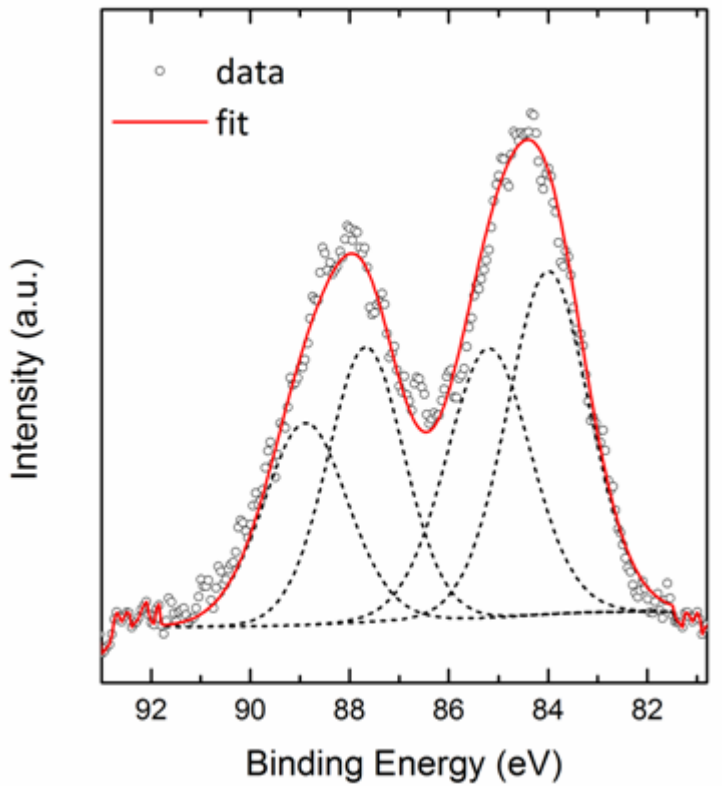

Fig. 9 XPS spectra of DNase 1 Au_{25}NC Au_{4f} spectra

4. Summary and Conclusions

In conclusion, we have been able to demonstrate the success of using DNase 1 to synthesize AuNCs of varied energy levels. We were able to synthesize both blue-emitting Au_8NCs and red-emitting Au_{25}NCs in addition to synthesizing DNase 1-stabilized AuNCs containing mixed populations of both Au_8 and Au_{25} clusters in a concentration-dependant fashion. However, further study is required to fully understand the mechanism of metal ion reduction and stabilization in protein-mediated NC synthesis.

5. References

1. Wang Q, Xu Y, Zhao X, Chang Y, Liu Y, Jiang L, Sharma J, Seo DK, Yan H. A facile one-step in situ functionalization of quantum dots with preserved photoluminescence for bioconjugation. J Am Chem Soc. 2007 May 23;129:6380–6381.
2. Mahmoudi AR, Shaban E, Ghods R, Jeddi-Tehrani M, Emami S, Rabbani H, Zarnani AH, Mahmoudian J. Comparison of photostability and photobleaching properties of FITC- and dylight488-conjugated herceptin. International Journal of Green Nanotechnology. 2011;3:264–270.
3. Landgraf D, Okumus B, Chien P, Baker TA, Paulsson J. Segregation of molecules at cell division reveals native protein localization. Nature Methods. 2012;9:480–482.
4. Alivisatos AP. Semiconductor clusters, nanocrystals, and quantum dots. Science. 1996;271:933–937.
5. Nirmal M, Dabbousi BO, Bawendi MG, Macklin JJ, Trautman JK, Harris TD, Brus LE. Fluorescence intermittency in single cadmium selenide nanocrystals. Nature. 1996;383:802–804.
6. Pinaud F, King D, Moore HP, Weiss S. Bioactivation and cell targeting of semiconductor CdSe/ZnS nanocrystals with phytochelatin-related peptides. Journal of the American Chemical Society. 2004;126:6115–6123.
7. Chevrier DM, Chatt A, Zhang P. Properties and applications of protein-stabilized fluorescent gold nanoclusters: short review. Journal of Nanophotonics. 2012;6:064504-1 to 06454-16.
8. Shang L, Dong SJ, Nienhaus GU. Ultra-small fluorescent metal nanoclusters: synthesis and biological applications. Nano Today. 2011;6:401–418.
9. Chen CT, Chen WJ, Liu CZ, Chang LY, Chen YC. Glutathione-bound gold nanoclusters for selective-binding and detection of glutathione S-transferase-fusion proteins from cell lysates. Chem Commun (Camb). 2009;48:7515–7517.
10. Hu D, Sheng Z, Gong P, Zhang P, Cai L. Highly selective fluorescent sensors for Hg(2+) based on bovine serum albumin-capped gold nanoclusters. Analyst. 2010;135:1411–1416.
11. Shang L, Dorlich RM, Brandholt S, Schneider R, Trouillet V, Bruns M, Gerthsen D, Nienhaus GU. Facile preparation of water-soluble fluorescent gold nanoclusters for cellular imaging applications. Nanoscale. 2011;3:2009–2014.
12. Hu L, Han S, Parveen S, Yuan Y, Zhang L, Xu G. Highly sensitive fluorescent detection of trypsin based on BSA-stabilized gold nanoclusters. Biosens Bioelectron. 2012;32:297–299.

13. Shang L, Dorlich RM, Brandholt S, Azadfar N, Nienhaus GU. Facile synthesis of fluorescent gold nanoclusters and their application in cellular imaging. Colloidal Nanocrystals for Biomedical Applications VII. 2012:8232.

14. Chan PH, Ghosh B, Lai HZ, Peng HL, Mong KK, Chen YC. Photoluminescent gold nanoclusters as sensing probes for uropathogenic escherichia coli. PLoS One. 2013;8:e58064.

15. Chen H, Li B, Wang C, Zhang X, Cheng Z, Dai X, Zhu R, Gu, Y. Characterization of a fluorescence probe based on gold nanoclusters for cell and animal imaging. Nanotechnology. 2013;24:055704.

16. Zhang H, Liu Q, Wang T, Yun Z, Li G, Liu J, Jiang G. Facile preparation of glutathione-stabilized gold nanoclusters for selective determination of chromium (III) and chromium (VI) in environmental water samples. Anal Chim Acta. 2013;770:140–146.

17. Hasobe T, Imahori H, Kamat PV, Ahn TK, Kim SK, Kim D, Fujimoto A, Hirakawa T, Fukuzumi S. Photovoltaic cells using composite nanoclusters of porphyrins and fullerenes with gold nanoparticles. J Am Chem Soc. 2005;127:1216–1228.

18. Zheng J, Nicovich PR, Dickson RM. Highly fluorescent noble-metal quantum dots. Annu Rev Phys Chem. 2007;58:409–431.

19. Zheng J, Zhang C, Dickson RM. Highly fluorescent, water-soluble, size-tunable gold quantum dots. Phys Rev Lett. 2004;93: 077402.

20. Kawasaki H, Hamaguchi K, Osaka I, Arakawa R. pH-dependent synthesis of pepsin-mediated gold nanoclusters with blue green and red fluorescent emission. Advanced Functional Materials. 2011;21:3508–3515.

21. Kennedy TA, MacLean JL, Liu J. Blue emitting gold nanoclusters templated by poly-cytosine DNA at low pH and poly-adenine DNA at neutral pH. Chem Commun (Camb). 2012;48:6845–6847.

22. Gwinn EG, O'Neill P, Guerrero AJ, Bouwmeester D, Fygenson DK. Sequence-dependent fluorescence of DNA-hosted silver nanoclusters. Advanced Materials. 2008;20:279–283.

23. Han B, Wang E. DNA-templated fluorescent silver nanoclusters. Analytical and Bioanalytical Chemistry. 2012;402:129–138.

24. Petty JT, Zheng J, Hud NV, Dickson RM. DNA-templated Ag nanocluster formation. Journal of the American Chemical Society. 2004;126:5207–5212.

25. Sengupta B, Springer K, Buckman JG, Story SP, Abe OH, Hasan ZW, Prudowsky ZD, Rudisill SE, Degtyareva NN, Petty JT. DNA templates for fluorescent silver clusters and I-motif folding. The Journal of Physical Chemistry C. 2009;113:19518–19524.

26. Zhang XD, Wu D, Shen X, Liu PX, Fan FY, Fan SJ. In vivo renal clearance, biodistribution, toxicity of gold nanoclusters. Biomaterials 2012;33:4628–46238.

27. Xie J, Zheng Y, Ying JY. Protein-directed synthesis of highly fluorescent gold nanoclusters. J Am Chem Soc. 2009;131:888–889.

28. Wei H, Wang Z, Yang L, Tian S, Hou C, Lu, Y. Lysozyme-stabilized gold fluorescent cluster: synthesis and application as Hg(2+) sensor. Analyst. 2010;135:1406–1410.

29. Le Guevel X., Daum N, Schneider M. Synthesis and characterization of human transferrin-stabilized gold nanoclusters. Nanotechnology. 2011;22:275103.

30. Liu CL, Wu HT, Hsiao YH, Lai CW, Shih CW, Peng YK, Tang KC, Chang HW, Chien YC, Hsiao JK, Cheng JT, Chou PT. Insulin-directed synthesis of fluorescent gold nanoclusters: preservation of insulin bioactivity and versatility in cell imaging. Angew Chem Int Ed Engl. 2011;50:7056–7060.

31. Chen Y, Wang Y, Wang C, Li W, Zhou H, Jiao H, Lin Q, Yu C. Papain-directed synthesis of luminescent gold nanoclusters and the sensitive detection of Cu(2+). J Colloid Interface Sci. 2013;396:63–68.

32. Garcia AR, Rahn I, Johnson S, Patel R, Guo J, Orbulescu J, Micic M, Whyte JD, Blackwelder P, Leblanc RM. Human insulin fibril-assisted synthesis of fluorescent gold nanoclusters in alkaline media under physiological temperature. Colloids Surf B Biointerfaces. 2013;105:167–172.

33. Wen F, Dong Y, Feng L, Wang S, Zhang S, Zhang X. Horseradish peroxidase functionalized fluorescent gold nanoclusters for hydrogen peroxide sensing. Analytical Chemistry. 2011;83:1193–1196.

34. Selvakannan PR, Swami A, Srisathiyanarayanan D, Shirude PS, Pasricha R, Mandale AB, Sastry M. Synthesis of aqueous Au core-Ag shell nanoparticles using tyrosine as a pH-dependent reducing agent and assembling phase-transferred silver nanoparticles at the air-water interface. Langmuir. 20041;20:7825–7836.

35. Chen TH, Tseng WL. (Lysozyme type VI)-stabilized Au8 clusters: synthesis mechanism and application for sensing of glutathione in a single drop of blood. Small. 2012;8:1912–1919.

List of Symbols, Abbreviations, and Acronyms

Au	gold
AuNC	gold nanocluster
HR-TEM	high-resolution tunneling electron microscopy
NC	nanocluster
QD	quantum dot
SEM	scanning electron microscopic
UV	ultraviolet
XPS	X-ray photoelectron spectroscopy

1 DEFENSE TECHNICAL
(PDF) INFORMATION CTR
DTIC OCA

2 DIRECTOR
(PDF) US ARMY RESEARCH LAB
RDRL CIO LL
IMAL HRA MAIL & RECORDS MGMT

1 GOVT PRINTG OFC
(PDF) A MALHOTRA

1 DIR USARL
(PDF) RDRL WMM A
A WEST

INTENTIONALLY LEFT BLANK.